

Live dynamics of *Dictyostelium* cofilin suggests a role in remodeling actin latticework into bundles

Hiroyuki Aizawa¹, Yoshio Fukui² and Ichiro Yahara^{1,*}

¹Department of Cell Biology, The Tokyo Metropolitan Institute of Medical Science, Honkomagome 3-18-22, Bunkyo-ku, Tokyo 113, Japan

²Department of Cell and Molecular Biology, Northwestern University Medical School, Chicago, Illinois, USA

*Author for correspondence (e-mail: yahara@rinshoken.or.jp)

SUMMARY

Cofilin, an indispensable, actin-regulating protein represents the 'cofilin family' of actin-binding proteins existing in a wide variety of organisms. Our previous and other *in vitro* studies have implied that cofilin can accelerate transformation of filamentous (F)-actin and α -actinin latticework into bundles, and overexpression of cofilin induces formation of F-actin bundles in *Dictyostelium*. Here we expressed an *Aequorea* green fluorescent protein (GFP)-*Dictyostelium* cofilin fusion protein in *Dictyostelium*, and observed the live dynamics to examine the physiological function of cofilin. We show that purified GFP-cofilin binds to actin filaments and decreases the apparent viscosity of actin solution in a similar manner to authentic *Dictyostelium* cofilin. Expressed GFP-cofilin exhibits normal actin-binding activities in the cytoplasm as represented by incorporation into the actin rods induced with dimethyl

sulfoxide. Free moving cells form a crown-like cortical structure on the dorsal surface, and GFP-cofilin exhibits dynamic assembly into actin bundles being formed beneath the cortex. During phagocytosis, GFP-cofilin accumulates into actin bundles formed in the region underlying the phagocytic cups. In cells chemotactically activated with cyclic AMP, GFP-cofilin exhibits a high level of accumulation in projecting leading edges. When the chemo-attraction is experimentally changed, the redistribution of GFP-cofilin towards the new pseudopod occurs in a matter of 30-60 seconds. These results demonstrate that cofilin plays a crucial role *in vivo* in rapid remodeling of the cortical actin meshwork into bundles.

Key words: Actin, Cell movement, Cofilin, *Dictyostelium*, Green fluorescent protein

INTRODUCTION

The actomyosin system generates biomechanical forces for various types of cell movements in eukaryotic cells such as phagocytosis, chemotactic movement, and cytokinesis. Unlike muscle contraction, amoeboid cell movement and other motile events performed by non-muscle cells appear to require an incessant rearrangement of the actin cytoskeleton (reviewed by Fukui and Yumura, 1986). Thus actin-regulating proteins are believed to play crucial roles in such dynamic cellular movements (reviewed by Stossel et al., 1985; Pollard and Cooper, 1986; Hartwig and Kwiatkowski, 1991; Vandekerckhove and Vancompernelle, 1992; Fukui, 1993). Cofilin has been proved to be essential for cell viability in *Saccharomyces cerevisiae* (Iida et al., 1993; Moon et al., 1993) and *Dictyostelium discoideum* (Aizawa et al., 1995). It is ubiquitously present in all eukaryotes examined so far, being structurally and functionally conserved (reviewed by Pollard, 1993; Sun et al., 1995; Moon and Drubin, 1995; Yahara et al., 1996). Together with its structural homologues, cofilin constitutes an actin-regulating protein family, the cofilin family, that includes cofilin (Nishida et al., 1984), destrin/actin-depolymerizing factor (ADF) (Bamburg et al., 1980; Nishida et al., 1985), actophorin (Cooper et al., 1986) and depactin (Mabuchi, 1981).

On the basis of structural similarity to the segment-1 domain of gelsolin (McLaughlin et al., 1993), a Ca^{2+} -independent binding mode of destrin to actin has been speculated (Hatanaka et al., 1996). It has been revealed that cofilin and destrin are functionally regulated in three ways: pH (Yonezawa et al., 1985; Hawkins et al., 1993), polyphosphoinositides (Yonezawa et al., 1990; Aizawa et al., 1995), and phosphorylation of the 3rd serine residue (Agnew et al., 1993; Moriyama et al., 1996). In higher eukaryotes, the dephosphorylation of cofilin is induced upon cellular activation by various stimuli (reviewed by Moon and Drubin, 1995; Yahara et al., 1996).

Cofilin binds both monomeric and polymerized forms of actin in a one-to-one molar ratio (Nishida et al., 1984). It severs and depolymerizes F-actin in a pH-dependent manner (Yonezawa et al., 1985). Overexpression of cofilin in *Dictyostelium* cells significantly increases the amount of F-actin but not that of monomeric actin, and induces numerous F-actin bundles, suggesting that cofilin severs, rather than depolymerizes, F-actin *in vivo* (Aizawa et al., 1996). Cofilin and actophorin have been shown *in vitro* to help transform F-actin and α -actinin latticework into bundles, and its severing activity is thought to contribute to this reorganization of F-actin (Maciver et al., 1991; Aizawa et al., 1996). In *Dictyostelium*, immunofluorescence microscopy showed that cofilin localizes

in the dorsal ruffling membrane but not in substrate adhesion plaques (Aizawa et al., 1995). An increase in F-actin bundles induced by the overexpression of cofilin is associated with stimulation of cell locomotion, suggesting a causal relationship between the two events (Aizawa et al., 1996).

Although cofilin has been speculated to be involved in remodeling of the actin cytoskeleton, to date little is known about the dynamics of cofilin in moving eukaryotic cells, particularly during specific motile activities. In this study, we investigated the live dynamics of cofilin in *Dictyostelium* by expressing a green fluorescent protein (GFP)-*Dictyostelium* cofilin fusion protein. A near real-time image analysis demonstrated that cofilin dynamically assembles into specific compartments of actin cytoskeleton in an order of seconds, suggesting a role in remodeling the actin framework from lattice to bundles in macropinocytosis, phagocytosis, cell division, and chemotaxis.

MATERIALS AND METHODS

Expression vectors

A control vector, pEXP, was constructed as follows. An extrachromosomal shuttle vector, pBIG (Uyeda et al., 1994) was digested with *NotI*, blunted by Klenow large fragment of DNA polymerase I, and self-ligated by T4 DNA ligase to construct a vector pBIGΔ*NotI*. Double stranded DNA was prepared by annealing two synthetic oligonucleotides, BNTX1 (GATCCGCGGCCGCTAAATAAATAAC) and BNTX2 (TCGAGTTATTTATTTAGCGGCCGCG), and the DNA was ligated into a plasmid pBsr2 (Sutoh, 1993) which had been digested with *Bam*HI and *Xho*I. The resultant plasmid was sequentially treated by *Hind*III, Klenow fragment, and *Xba*I. The excised 0.9 kbp fragment was ligated into the pBIGΔ*NotI*, which had been pretreated sequentially with *Bam*HI, Klenow fragment, and *Xba*I. The resultant extrachromosomal vector, pEXP, contains *Bam*HI, *NotI*, and *Xho*I restriction sites between an actin 15 promoter and an actin 8 terminator. An expression vector for GFP, pGFP, was constructed as follows. An S65T-GFP cDNA was amplified by PCR using two synthetic oligonucleotides, GFP-F (AAATGGATCCGAGTAAAGGAGAAGAAGACTT) and GFP-R (AAAACCTCGAGTTAGTCGACTTTGTATAGTTCATCCAT), as primers from a template plasmid containing an S65T-GFP coding sequence (a gift from Dr R. Y. Tsien, University of California, La Jolla, CA). The amplified cDNA was digested with *Bam*HI and *Xho*I, and ligated into pEXP which had been treated with *Bam*HI and *Xho*I. The resultant plasmid, pGFP, expresses a S65T-GFP protein with two additional amino acid residues (Asp and Pro) just after the initiation Met and two additional amino acid residues (Val and Asp) on the carboxyl terminus. We also constructed a vector for expression of (His)₆-tagged GFP, pHGFP, by using a synthetic oligonucleotide primer, HGFP-F (AAATGGATCCGATCATCATCATCATAGTAAAGGAGAAGAAGACTT), instead of the primer GFP-F as described above. An expression vector for GFP-cofilin was constructed as follows. cDNA was amplified by PCR using two synthetic oligonucleotides CA1 (AAAATGGATCCCTCTTCAGGTATTGCTTTA) and CT1 (AAAATCTCGAGTCAAATTATTTAGATTTT) from a template plasmid pDDCOF2 (Aizawa et al., 1995). The amplified cDNA was treated with *Bam*HI and *Xho*I and ligated with pBsr2 that had been pretreated with *Bam*HI and *Xho*I. The resultant plasmid, pCA1, was used as a template for the amplification of cofilin cDNA by PCR using two synthetic oligonucleotides, CA1 and M13 reverse primers, as the primers. The cofilin cDNA was blunted by a Klenow large fragment of DNA polymerase I, and then treated with *Sal*I. The cDNA was ligated into pGFP which had been treated sequentially by *Xho*I, Klenow fragment, and *Sal*I. The resultant plasmid, pGCOF, contains an artificial GFP-cofilin

fusion gene consisting of an actin 15 promoter, an initiation Met codon followed by six nucleotides encoding Asp and Pro, in-frame GFP-cofilin cDNA, and two tandem repeats of actin 8 terminator. We also constructed a vector for the expression of (His)₆-tagged GFP-cofilin, pHGCOF, by inserting the cofilin cDNA into the plasmid pHGFP instead of the pGFP as described above. The expression plasmids, pEXP, pCOF, pGFP, pGCOF, and pHGCOF, were separately introduced into the Ax2 cells by electroporation and the transformed cells were selected in HL5 medium containing 10 μg/ml G418 as described before (Aizawa et al., 1995).

Protein purification

Rabbit skeletal muscle actin was prepared according to the method of Spudich and Watt (1971) with some modifications (Aizawa et al., 1995). Authentic cofilin was purified from Ax2 cells as described previously (Aizawa et al., 1995). The (His)₆-tagged GFP-cofilin was prepared from Ax2 cells carrying pHGCOF as follows. The transformed cells (2.5 ml in packed volume) were lysed by sonication in 25 ml of 10 mM Tris-Cl, pH 7.5, containing protease inhibitors (1 mM PMSF, 10 μg/ml leupeptin, and 1% aprotinin). After centrifugation, the pellet was suspended in 25 ml of 5 mM imidazole containing 500 mM NaCl ('crude extract'). The extract was mixed with 0.5 ml of His-Bind Metal chelation resin which immobilized the Ni²⁺ (Novagen, Madison, WI). The resin was washed three times with 10 mM Tris-Cl, pH 7.5, 10 mM imidazole, and 500 mM NaCl, and packed in a tube (8 mm × 300 mm). The adsorbed proteins were eluted by 250 mM imidazole in 10 mM Tris-Cl, pH 7.5, and 500 mM NaCl. The (His)₆-tagged GFP-cofilin fraction could be identified with the naked eye by its green color. The eluted material was then separated by hydroxyapatite column chromatography by 0.5 ml of a 10-200 mM linear gradient of NaH₂PO₄. Fractions containing GFP-cofilin were dialyzed against 20 mM Mes, pH 6.85, and 1 mM EGTA. The purity was more than 95% as determined by SDS-PAGE.

Biochemical characterization

Subcellular fractionation was performed as described previously (Aizawa et al., 1996). Low shear rate apparent viscosity was measured with a miniature falling ball system at 25°C using 50 μl capillary tubes (Clay Adams, Parsippany, NJ) (Aizawa et al., 1995).

Cells and cultures

D. discoideum Ax2 cell line (clone 214) was cultured on a plastic plate as previously described (Aizawa et al., 1995). At late exponential phase, the medium was replaced with Bonner's salt solution (Bonner, 1947). The vegetative stage amoebae were collected by scraping off the bottom of the plate with a silicone rubber policeman (Fukui and Inoué, 1997). Stationary stage amoebae were collected after 2-3 hours of incubation at 22°C. Aggregation stage amoebae were prepared by incubating a confluent culture in Bonner's solution for 18 hours at 22°C before scraping off.

Phagocytosis

The amoebae were pre-fixed with 2% formaldehyde for 10 minutes and washed three times with phosphate buffered saline (PBS: 138 mM NaCl, 2.5 mM KCl, 8 mM Na₂HPO₄, 1.5 mM KH₂PO₄, pH 7.2). The fixed amoebae were mixed with live vegetative stage Ax2 amoebae at a 1:1 ratio. The samples were prepared by the agar-overlay method (Fukui et al., 1986) and incubated for one hour before fixation. The sample was then processed for immunofluorescence localization (see below). For the live observation of phagocytosis, *Saccharomyces cerevisiae* were mixed with vegetative stage amoebae and incubated for about an hour before image recording.

Fluorescence microscopy

The fluorescence staining of F-actin was performed using rhodamine-phalloidin (rh-ph) as described previously (Aizawa et al., 1995). The stained cells were observed and recorded under a confocal laser scanning

microscope (MRC 600; Bio-Rad Laboratories, Japan) (Aizawa et al., 1996). Double-staining of cofilin and actin by the agar overlay technique was performed as previously reported (Fukui et al., 1986). Briefly, the samples were fixed with methanol containing 1% formaldehyde for 5 minutes at -15°C , and washed with PBS three times for 5 minutes each. A 1:1 mixture of the primary antibodies (a rabbit anti-*Dictyostelium* cofilin, 1:25, and a mouse monoclonal anti-*Dictyostelium* actin, ATCC HB-80, 1:1) was applied to the samples and incubated for 30 minutes at 36°C . After washing, a 1:1 mixture of the secondary antibodies (FITC-goat anti-rabbit IgG, Sigma F-1262, 1:25 and TMRITC-goat anti-mouse, Southern Biotechnology Associates #1030-30; 1:50) was applied to the samples and incubated for 30 minutes at 36°C . The samples were mounted with a 1:2:4 mixture of polyvinyl alcohol, glycerol, and PBS containing 1% (w/v) of an anti-oxidant DABCO (diazabicyclo[2.2.2]octane) (Aldrich Chemical Co., Milwaukee, WI). For fluorescence microscopy, a Zeiss Axioskop-50 (Carl Zeiss, Inc., Thornwood, NY) equipped with a $\times 63$, NA 1.4 plan apo objective was used. The image was recorded through a cooled CCD camera (model PXL; Photometrics, Tucson, AZ) equipped with Kodak KAF1400 chips.

Light microscope observation of live cells

The live cells were observed under an Olympus IMT-2 inverted microscope using an $\times 100$ plan apochromat objective lens (S-Plan Apo, NA 1.4). The microscope was attached to a real time laser confocal microscope system 'Insight Plus-IQ' (Meridian Instruments Far East, Tokyo, Japan) equipped with a 500 mW argon laser and a B-cube for 488 nm excitation. The laser power was attenuated to 10–20 mW for observing GFP and GFP-cofilin expressing amoebae. The raw images were acquired with an 8-bit depth of gray level using the Meridian I-Plus IQ program and saved as Tiff files onto the hard drive. For DMSO treatment and cAMP stimulation, Ax2 cells were suspended in a MCM buffer (20 mM Mes, 0.2 mM CaCl_2 , 2 mM MgCl_2 , pH 6.85) and plated on a poly-L-lysine-coated 35 mm glass-bottomed culture dish (MattTek Corp., Ashland MA). For high-resolution observation of live amoebae, we employed the agar-overlay method for live cells (Fukui and Inoué, 1991, 1997). Briefly, a 100 μl sample of cell suspension containing about 200 amoebae was dropped in the center of a 22 mm \times 22 mm² glass coverslip (no. 1.5, 170 μm thick; Corning Glass Works, Corning, NY) and overlaid with a small piece of agarose film (170 μm thick, 5 mm \times 5 mm²). The sample was turned over and placed on a 22 mm \times 40 mm² slide glass supported by a square-shaped 170 μm thick spacer made of Whatman no. 541 filter paper, and sealed with VALAB (a 1:1:1 mixture of vaseline, lanolin and bee's wax). Since GFP or GFP-cofilin expressing cells are sensitive to the excitation, the laser power was attenuated to 20 mW and a 10%-transmission neutral density (ND) filter was installed. To acquire images, the samples were exposed for 0.5 seconds at 5 second intervals. Under these conditions, the amoebae continued normal migration for many hours.

Electron microscope observation

Cells grown on glass coverslips were fixed with 2.5% glutaraldehyde in PBS at 25°C for 30 minutes. After dehydration through an ethanol series (5 minutes each of 30, 50, 80, and 95%), then 100% ethanol (3 \times 5 minutes), and finally 100% t-butanol (3 \times 5 minutes), the samples were chilled at -20°C for 10 minutes before freeze drying. The samples coated with gold were examined with a scanning electron microscope (S4500, Hitachi, Tokyo, Japan).

Imaging

The measurement of gray scale intensity was done using a Line Intensity Scan menu of Image-1/AT (Universal Imaging Corp., West Chester, PA). The image panels were made by using Photoshop (Adobe Systems, Inc., Mountain View, CA) and printed using a Pictography 3000 printer (Fuji Corp., Tokyo).

Other methods

Protein concentration was determined by the Bio-Rad protein assay

system (Bio-Rad Laboratories, Richmond, CA) using goat γ -globulin as a standard. SDS-PAGE was carried out according to the method of Laemmli (1970) with a 10–20% gradient gel (Multigel 10/20; Daiichi Pure Chemicals Co., Tokyo, Japan). Molecular mass markers for SDS-PAGE (Bio-Rad Laboratories, Hercules, CA) contained myosin (200 kDa), β -galactosidase (116 kDa), phosphorylase b (97 kDa), bovine serum albumin (66 kDa), ovalbumin (45 kDa), carbonic anhydrase (31 kDa), trypsin inhibitor (21.5 kDa), and lysozyme (14.4 kDa). Gels were stained with Coomassie Brilliant Blue (CBB) R-250. Western blotting (Towbin et al., 1979) was performed using a rabbit anti-cofilin antiserum and a horseradish-conjugated goat anti-rabbit IgG (Aizawa et al., 1996).

RESULTS

Expression of GFP-*Dictyostelium* cofilin

We constructed an extrachromosomal vector, pGCOF, in order to express a chimeric protein made of GFP and *Dictyostelium* cofilin in *Dictyostelium* (Fig. 1). For expressing GFP and GFP-cofilin, plasmids pGFP and pGCOF were loaded into Ax2 cells by electroporation, and transformants were selected by G418. Each electroporation yielded about a hundred colonies, and we used mixed colonies within 3 weeks after electroporation for all the experiments described in this paper. The growth, locomotion, and development were apparently normal in the transformants (data not shown). The protein compositions of total cell homogenate, precipitate and supernatant fractions were almost same in pGFP (data not shown) and pGCOF transformants, as resolved by SDS-PAGE (Fig. 2A). Western blot analysis revealed the presence of a 43 kDa protein reactive with anti-cofilin antibody in the pGCOF transformant in addition to the endogenous 15 kDa cofilin (Fig. 2A). Since the purified 43 kDa protein fluoresced (data not shown), we determined that it was GFP-cofilin fusion protein, whose estimated molecular weight was 42,519. The amount of GFP-cofilin was about 10% (mol/mol) of the total cofilin in the transformed cells (Fig. 2A). Thirty to 40% of the GFP-cofilin was recovered in the precipitate fraction, as was the authentic cofilin (Fig. 2A).

Biochemical property of S65T-GFP-*Dictyostelium* cofilin fusion protein

To purify GFP-cofilin, we expressed (His)₆-tagged GFP-cofilin in Ax2 cells with a vector pHGCOF. The 43 kDa protein was purified from the cell extract by Ni^{2+} -resin column chromatography, followed by hydroxyapatite column chromatography (Fig. 2B).

We attested whether the GFP-cofilin fusion protein

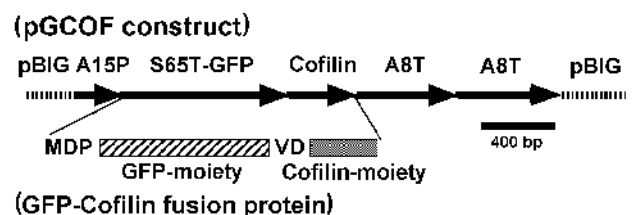
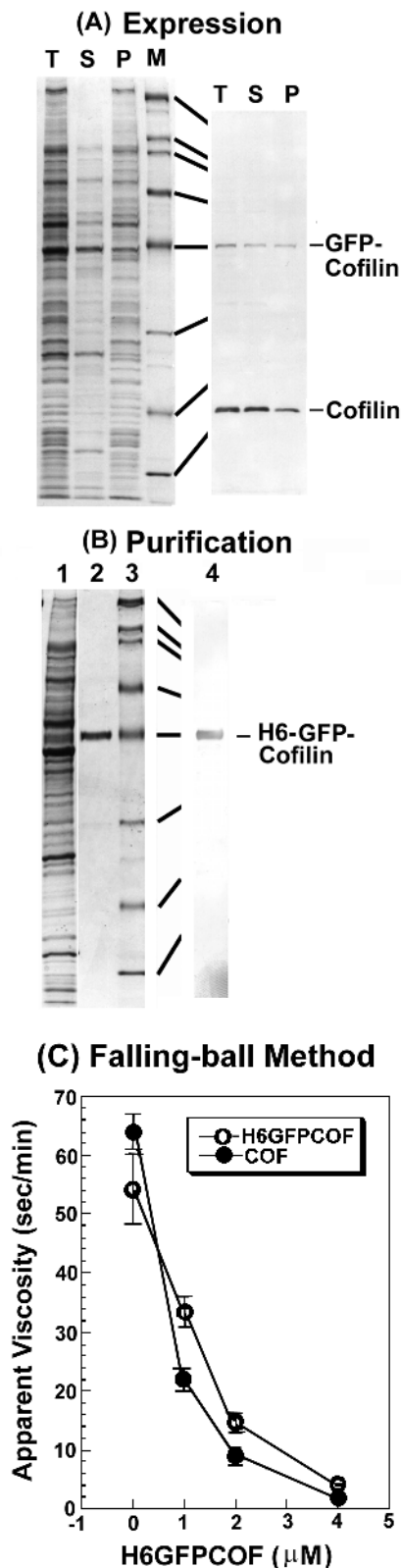


Fig. 1. Schematic diagram of S65T-GFP-*Dictyostelium* cofilin DNA in pGCOF, and its protein product (below). A15P, actin 15 promoter; A8T, actin 8 terminator; M, methionine; D, aspartic acid; P, proline; V, valine.

maintains the activity of the natural cofilin. First, we show that the GFP-cofilin decreases the apparent viscosity of actin filaments in a dose-dependent manner (Fig. 2C). The biochemical activities of authentic cofilin and GFP-cofilin, both of which were purified from *Dictyostelium* Ax2 cells, are indis-

tinguishable. Next, we examined the F-actin-binding activity of GFP-cofilin. We have found that the fusion protein is capable of co-sedimenting with F-actin by centrifugation in dose-dependent and saturatable manners (data not shown). In the presence of an excess amount of GFP-cofilin, almost equimolar cofilin was co-sedimented with F-actin.



Visualization of GFP and GFP-cofilin in live cells

Control Ax2 cells carrying a mock vector, pEXP, do not exhibit any background fluorescence detectable with 488-nm excitation (data not shown). The observed fluorescence therefore demonstrates the level of GFP or GFP-cofilin being expressed in the amoebae. Since GFP-cofilin and (His)₆-tagged GFP-cofilin behave similarly in cells, we described only GFP-cofilin in this paper. First, we examined the general mode of dynamics of GFP and GFP-cofilin in live, stationary stage cells using the agar-overlay method (Fig. 3). This method provides better spatial resolution due to nearly two-dimensional morphology (Fukui et al., 1986), and there is no adverse effect caused by compression intrinsic to this technique (Fukui and Inoué, 1991, 1997). GFP shows a global, diffuse distribution in the cytoplasm during the entire cell cycle including cytokinesis and post-mitotic locomotion (Fig. 3A). The fluorescence intensity of GFP is relatively high at the central region of the cell, apparently due to convexity or another. We have also occasionally noticed somewhat higher intensity at the pseudopod (Fig. 3A-d), but the frequency as well as the intensity was not conspicuous.

In contrast, we observed a significant accumulation of GFP-cofilin at the leading edges of protruding pseudopods (Fig. 3B). The image panel (left) indicates that GFP-cofilin exhibits the highest degree of accumulation in pseudopods when they fully develop (d), and rapidly dissipate when they retract (e). This feature was unambiguously demonstrated by a line intensity scan of a pseudopod showing a cycle of projection and retraction during the observation (right). These data demonstrate that GFP-cofilin rapidly accumulates in the developing pseudopod (a'-b'), integrated into an intense, sharp fluorescent band (d'), and this structure loosened when the pseudopod starts retracting (e'). This evidence demonstrates that the observed accumulation of GFP-cofilin is attributed to the cofilin moiety of the fusion protein but not to the GFP moiety. The data also showed a diffuse fluorescence of GFP-cofilin in the cytoplasm

Fig. 2. Biochemical property of GFP-*Dictyostelium* cofilin.

(A) Expression of the GFP-cofilin. Ax2 cells were transformed with a vector, pGCOF, for expression of GFP-cofilin. Total cell homogenate (T) was fractionated into supernatant (S) and precipitate (P) by centrifugation. M, marker proteins. Left panel, CBB staining; right panel, western blotting with anti-cofilin antiserum. (B) Purification of (His)₆GFP-cofilin. The crude extract was prepared from Ax2 cells expressing (His)₆-tagged GFP-cofilin. (His)₆GFP-cofilin was affinity purified by Ni²⁺-immobilized His-Bind resin, and further fractionated by hydroxyapatite column chromatography. Lane 1, crude extract; lanes 2 and 4, hydroxyapatite fraction; lane 3, marker proteins. Lanes 1-3, CBB staining; lane 4, western blotting with anti-cofilin antiserum. (C) Effects of GFP-cofilin and authentic cofilin on low shear viscosity of actin solution as determined by the falling ball method. Actin monomer (7 μM) was polymerized at 25°C for 2 hours in 1× F buffer (20 mM Mes, pH 6.85, 1 mM EGTA, 0.5 mM ATP, 1 mM MgCl₂, and 50 mM KCl) in the presence of various amounts of the GFP-cofilin or authentic cofilin.

that likely manifests free GFP-cofilin unbound to F-actin bundle or mesh.

Assembly of GFP-cofilin into actin rods induced by DMSO

Treatment of amoebae with 10% dimethyl sulfoxide (DMSO)

brings in formation of nuclear actin rods of F-actin in a reversible manner (Fukui, 1978). We have previously shown that the formation of the nuclear rods is attributed by redistribution of cofilin from the cytoplasm into the nucleus, where it assembles into cofilin-actin rods (Aizawa et al., 1995). To examine whether GFP-cofilin maintains this activity in live

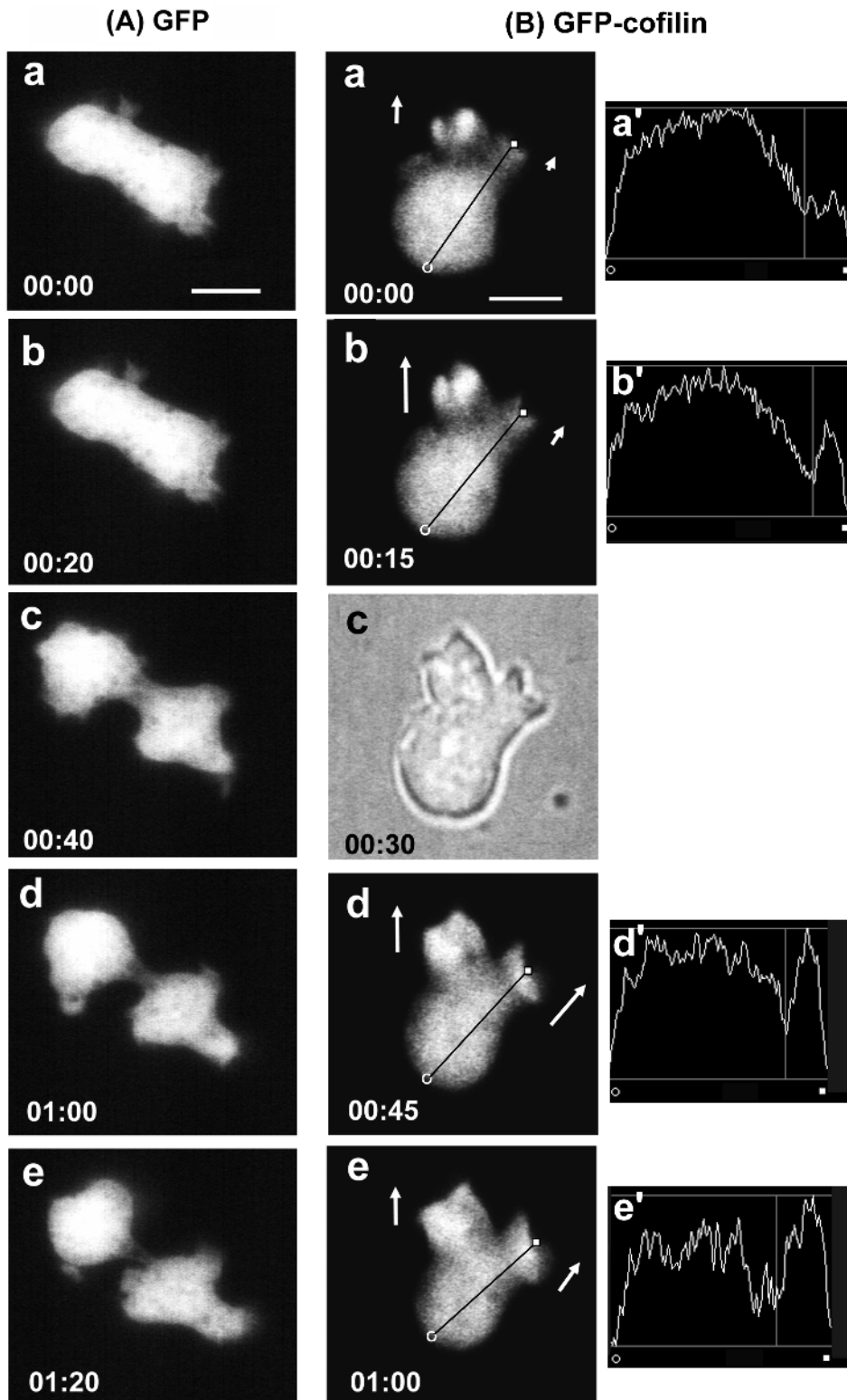


Fig. 3. Distribution of GFP and GFP-*Dictyostelium* cofilin in live *Dictyostelium* cells during general motile activity. (A) Distribution of GFP in a GFP-expressing cell as a control. This amoeba completed cytokinesis during observation and GFP shows only a diffuse pattern of distribution throughout the life cycle. Note that GFP does not accumulate into the cortex or pseudopodia. (a and b) Early cytokinesis, (c and d) mid cytokinesis, (e) late cytokinesis. (B) Distribution of GFP-cofilin during the random migration. Fluorescence (a,b,d,e) and bright-field (c) images acquired every 15 seconds. The direction of migration is towards the top. The arrows with different lengths indicate the pseudopod stage: (a) initiation, (b) development, (c) full extension, and (e) retraction. (a'-e') The line intensity scan of the fluorescence intensity measured on the line overlaid on corresponding images in a,b,d,e. Note that GFP-cofilin rapidly accumulates into extending pseudopod (a'-b'), shows a intense band when it fully develops (d'), and the fluorescence band loosens when the pseudopod starts to retract (e'). Time scale, minutes:seconds. Bars, 5 μ m.

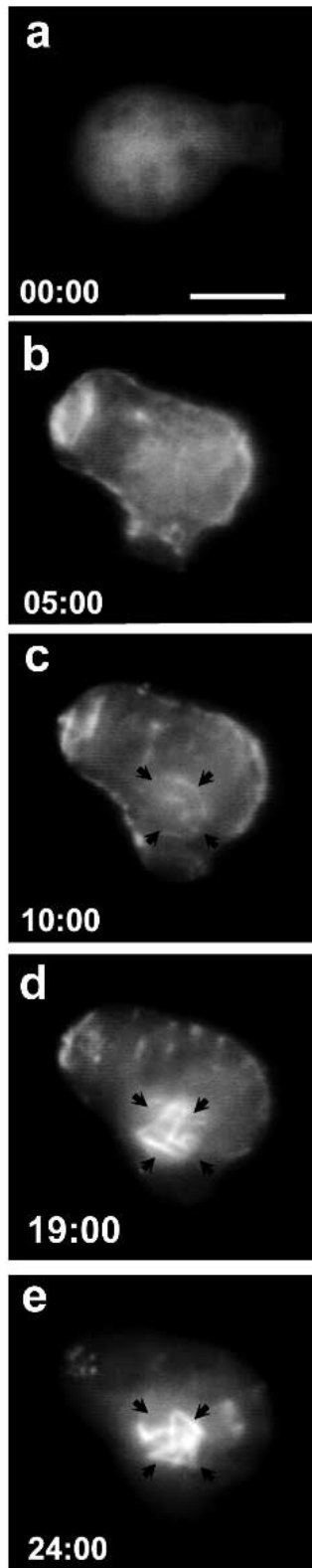


Fig. 4. Dynamic redistribution of GFP-cofilin in a DMSO-treated live cell. The GFP-cofilin expressing cell was treated with 10% (v/v) DMSO at time 0. During the initial 5 minutes (b), cofilin shows a cortical accumulation. Cofilin changes its organization in the subsequent 20 minutes (c,d), and eventually accumulates into the nucleus forming the actin-cofilin rods (e). Arrows, nuclear envelope. Time scale, minutes:seconds. Bar, 5 μ m.

cells, we first tested its ability to form the DMSO-induced actin-cofilin rods (Fig. 4). Within 5 minutes after the treatment with 10% (v/v) DMSO, GFP-cofilin was assembled into fibrous structures in the cortex (Fig. 4b), which also consist of F-actin as shown by double-staining immunofluorescence (data not shown). Then the fibrils fragmented, moved to the perinuclear region and transiently formed ring-shaped filamentous bundles around the nuclear envelope (Fig. 4c). The cofilin and actin complex was ultimately transported into the nucleus, and the number, length, and thickness of the cofilin-actin rods increased gradually between 10 and 24 minutes after the treatment. By 24 minutes after the DMSO treatment, almost all the cofilin-actin containing structures in the cytoplasm disappeared (Fig. 4e). This result not only confirmed that GFP-cofilin brings the cofilin ability into full play in vivo, but also demonstrated for the first time that cofilin sequentially associates with changing actin forms i.e. cytoplasmic and cortical fibrils, perinuclear filamentous bundles, and intranuclear rods.

Dynamic assembly of GFP-cofilin into specific actin-containing structures

Cortical crown-like protrusions

Vegetative *Dictyostelium* amoebae protrude crown-like lamellipodia (de Hostos et al., 1991). It has been recently indicated that this cortical structure (Fig. 5A) may be involved in macropinocytosis (Hacker et al., 1997). The rhodamine-phalloidin staining reveals that the bundles of F-actin underlie the crown along its marginal edges like purse strings (Fig. 5B). The cells fasten the purse strings of the crown, and rapidly retract the protrusions like a sea anemone (Fig. 5C). This sequential movement takes approximately one minute to complete. Live observation demonstrates that GFP-cofilin transiently co-assembles into the actin bundles at the marginal edges of the crown during the closure of the purse strings (Fig. 5C). We did not detect significant accumulation of GFP-cofilin at the crown during the protruding process.

Phagocytic cups

When vegetative cells contact their putative foods such as yeast and dead *Dictyostelium* cells, they protrude lamellipodia either side of the foods in order to engulf them, forming phagocytic cups. Double-staining immunofluorescence reveals that cofilin co-assembles with F-actin into bundles at the phagocytic cup (Fig. 6A). The live observation demonstrates that GFP-cofilin accumulates at the phagocytic cup (Fig. 6B). Although the intensity at the cup is not as discrete as that shown by immunofluorescence (Fig. 6A), the intensity measurement clearly demonstrates that the intensity at the cup is several times higher than the rest of the cell body (Fig. 6B, right panels). Note that the GFP-cofilin illustrates the distribution of both free and cytoskeleton-bound cofilin, whereas the immunofluorescence staining specifically demonstrates the localization of a cytoskeleton-bound, non-extractable form of cofilin.

Polar lamellae, but not cleavage furrow

The dividing *Dictyostelium* amoeba has two discrete F-actin-containing structures, the cleavage furrow and the polar lamellae (Fukui and Inoué, 1991). We found that cofilin accumulates at the polar lamellae, but not at the cleavage furrow,

as shown by immunofluorescence (Fig. 7A). The live observation of a single dividing cell clearly demonstrates that GFP-cofilin assembles into the polar lamellae only when they develop and rapidly dissipates when they retract (Fig. 7B). We examined more than 10 dividing cells but never detected any significant accumulation of GFP-cofilin at the cleavage furrow or the midbody. We do not know the reason why cofilin does not associate with F-actin forming the contractile ring, but this observation is consistent with the absence of α -actinin from the contractile ring in this organism (Fukui, 1993).

Anterior pseudopod produced by chemotactically activated amoebae

Under starvation stress, *Dictyostelium* cells start to move chemotactically to the chemoattractant, cAMP, within 6 hours (Bonner, 1947; Gerisch et al., 1995). Immunofluorescence demonstrates that, in chemotactically activated cells, cofilin coassembles with F-actin in their leading edge (Fig. 8A). We

also demonstrate that GFP-cofilin accumulates at the leading edge projecting towards the source of cAMP which is applied by a micropipette (Fig. 8B-D). This assembly occurs rapidly and GFP-cofilin exhibits the highest level of accumulation in the developing pseudopod within 30-60 seconds (Fig. 8C,D). This cofilin-actin structure seems to represent a distinctive form of actin bundle as previously reported (Yumura et al., 1984; Fig. 6-d). The above evidence, in conjunction with accompanying data described in this paper, demonstrate that cofilin assembles into the actin cytoskeleton in a temporally and spatially coordinated manner. These dynamics are surprisingly swift and sophisticated, and suggest that known biochemical properties such as pH-sensitivity and/or phosphorylation/dephosphorylation may also underly the *in vivo* properties revealed in the present study. Finally, we suggest that, in conjunction with the previous evidence that a cofilin gene knockout is lethal (Aizawa et al., 1995), cofilin plays an essential role in remodeling the actin latticework into bundles in action.

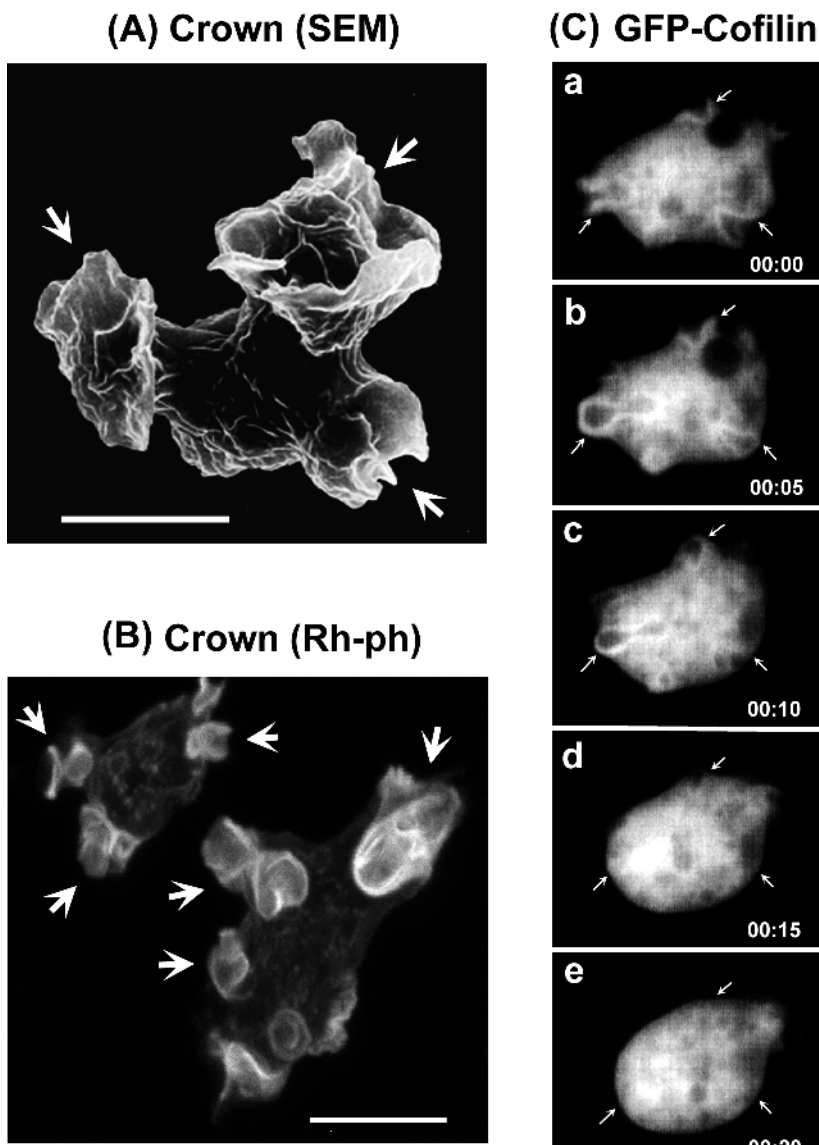


Fig. 5. Dynamic assembly of GFP-cofilin into crown-like cortical structures. (A) A scanning electron micrograph (SEM) showing the crown. (B) A fluorescence micrograph showing F-actin localization in the crown as revealed by Rh-ph staining. Arrows in A and B indicate typical crowns. (C) Dynamic distribution of GFP-cofilin in the crown as revealed by live cell observation. Arrows indicate the rapid reorganization of cofilin occurring in the crown within the 5 seconds' interval. Time scale, minutes:seconds. Bars, 5 μ m.

DISCUSSION

Various stresses such as DMSO treatment and heat shock induce the formation of intranuclear and/or cytoplasmic bundles of actin filaments, called actin rods, in a wide variety of cells (Fukui, 1978; Iida and Yahara, 1986; Iida et al., 1986). These actin rods contain cofilin and/or its homolog, destrin/ADF, as their major components (Nishida et al., 1987; Ono et al., 1993). Although it has been established that proteins

of the cofilin family depolymerize F-actin in a pH-dependent manner (Yonezawa et al., 1985; Hawkins et al., 1993), the above evidence indicates that it is not the only activity of this actin-regulating factor. In fact, we have previously shown that the overexpression of cofilin in *Dictyostelium* does induce the formation of thick actin bundles (Aizawa et al., 1996).

Interestingly, our recent studies have demonstrated in vitro that cofilin facilitates transformation of actin latticework into bundles, probably by producing short filaments (Aizawa et al.,

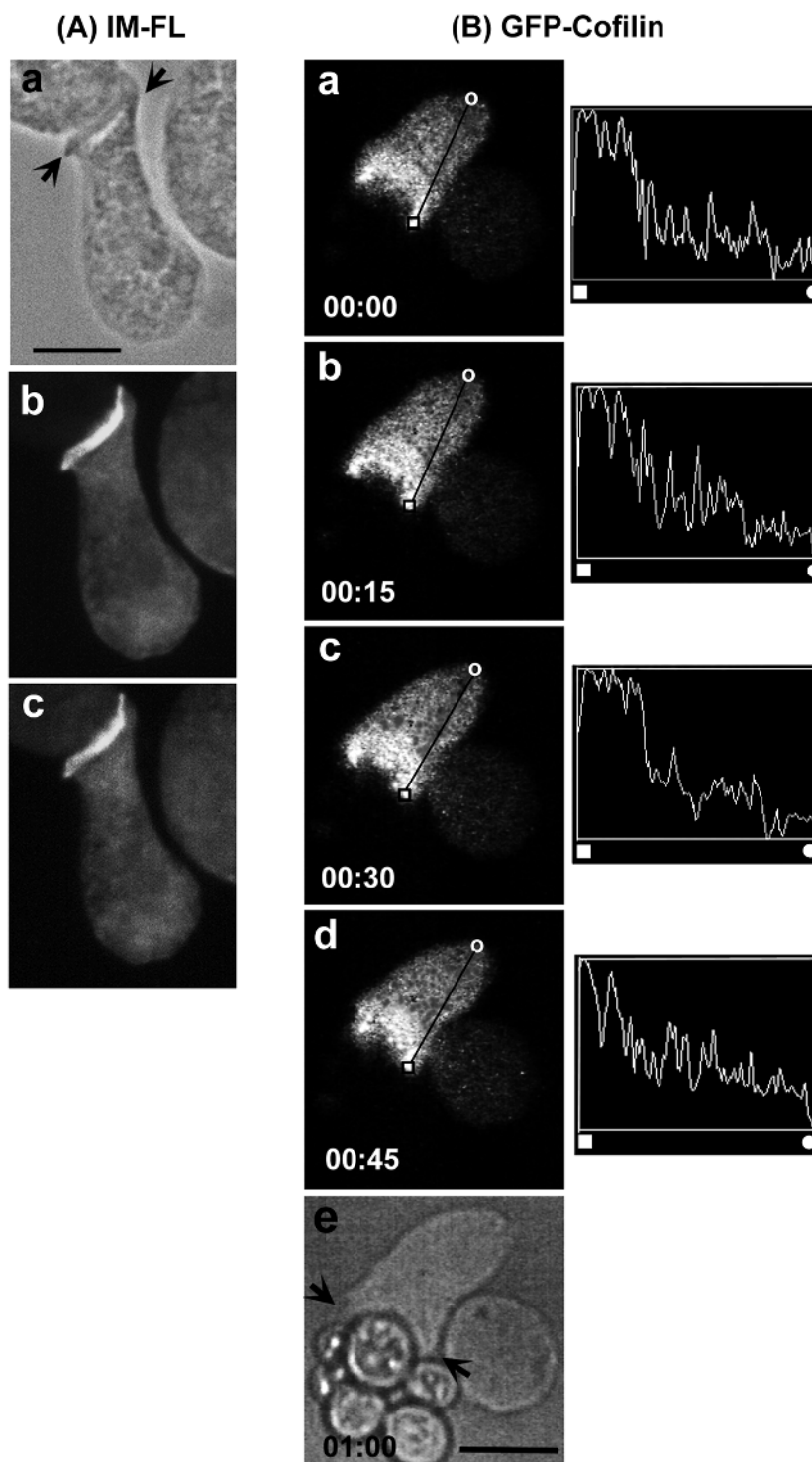


Fig. 6. Immunofluorescence localization of cofilin and live dynamics of GFP-cofilin during phagocytosis. (A) Phase-contrast (a) and double-staining fluorescence micrographs (b,c) showing an accumulation of cofilin in the phagocytic cup. Note that the localization of cofilin (c) is very similar to that of actin (b). (B) Distribution of GFP-cofilin in a live GFP-cofilin expressing cell endocytosing yeast cells. Note that cofilin shows the highest accumulation in the phagocytic cup and exhibits a dynamic change occurring within the 15 seconds' interval as illustrated by the line intensity scan (right). The black line connecting a white square and a white circle (a-d) shows the scanned line. Arrows, phagocytic cup. Time scale, minutes:seconds. Bars, 5 μ m.

1996). This model is consistent with the observation by Nishida et al. (1984), showing that cofilin severs actin filaments. Based on this evidence, we postulated that the actin-severing activity of cofilin may play a physiological role in the remodeling of the actin latticework (Aizawa et al., 1996).

However, the grounds for this hypothesis were based on unnatural, drastic conditions, such as the DMSO treatment or the overexpression of cofilin. In the present study, we observed the in situ molecular dynamics of cofilin using a GFP-cofilin fusion protein as a probe, particularly with regard to its asso-

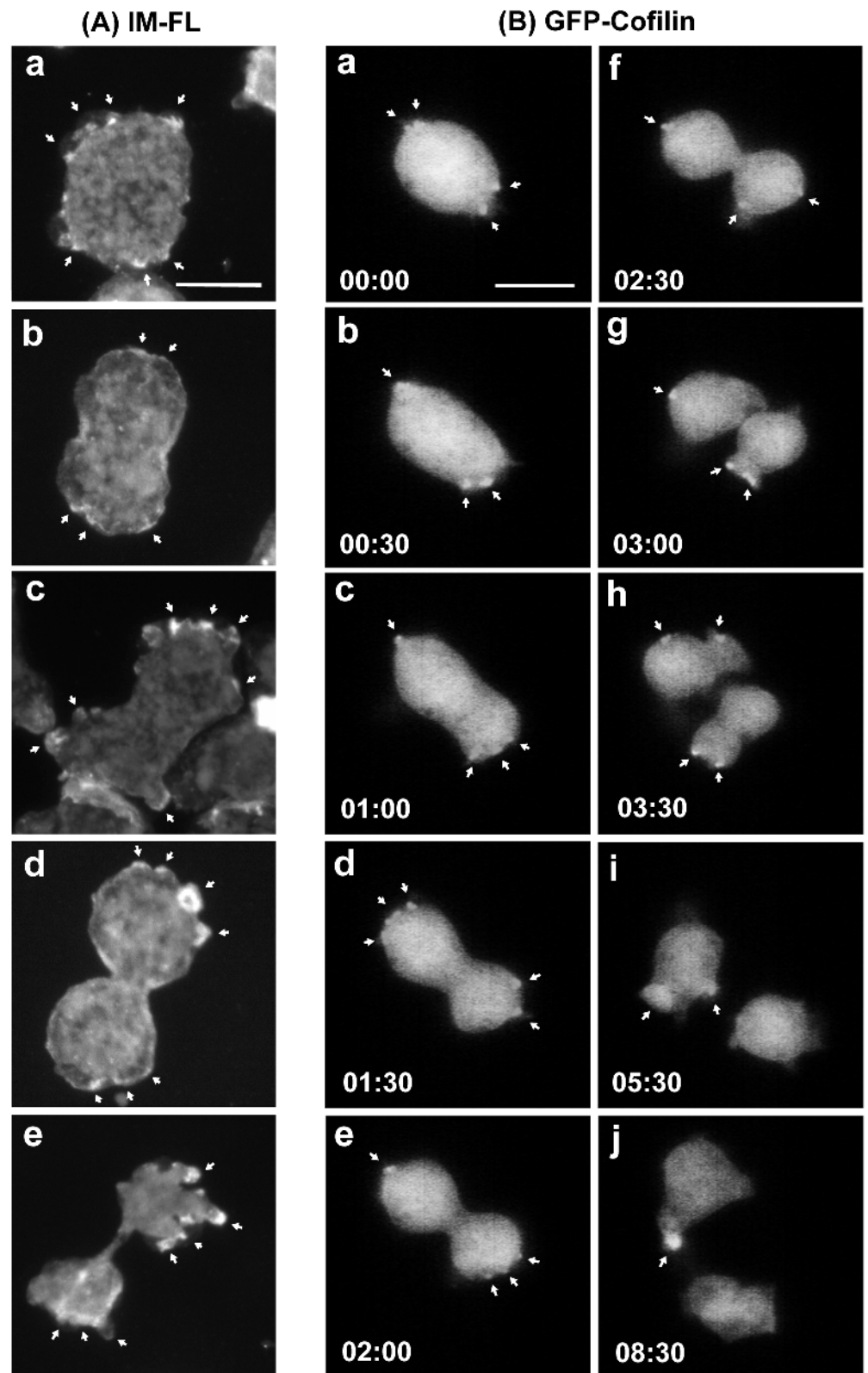


Fig. 7. Immunofluorescence localization of cofilin and live dynamics of GFP-cofilin during cytokinesis. (A) Immunofluorescence (IM-FL) localization of cofilin in fixed amoebae. (a) Anaphase, (b) early cytokinesis, (c) middle of cytokinesis, (d) late cytokinesis, (e) end of cytokinesis. Note that cofilin exhibits the highest localization in the polar lamellae (white arrows) but does not show accumulation in the cleavage furrow. (B) Live dynamics of GFP-cofilin during cytokinesis. (a) Anaphase, (b and c) early cytokinesis, (d and e) mid cytokinesis, (f) late cytokinesis, (g) end of cytokinesis, (h-j) separation of the daughter cells. Consistent with the immunofluorescence data, GFP-cofilin accumulates in the polar lamellae (white arrows) but not in the cleavage furrow. Note the dynamics of redistribution of cofilin shown in this live observation. Arrows, polar lamellae and pseudopodia. Time scale, minutes:seconds. Bars, 5 μ m.

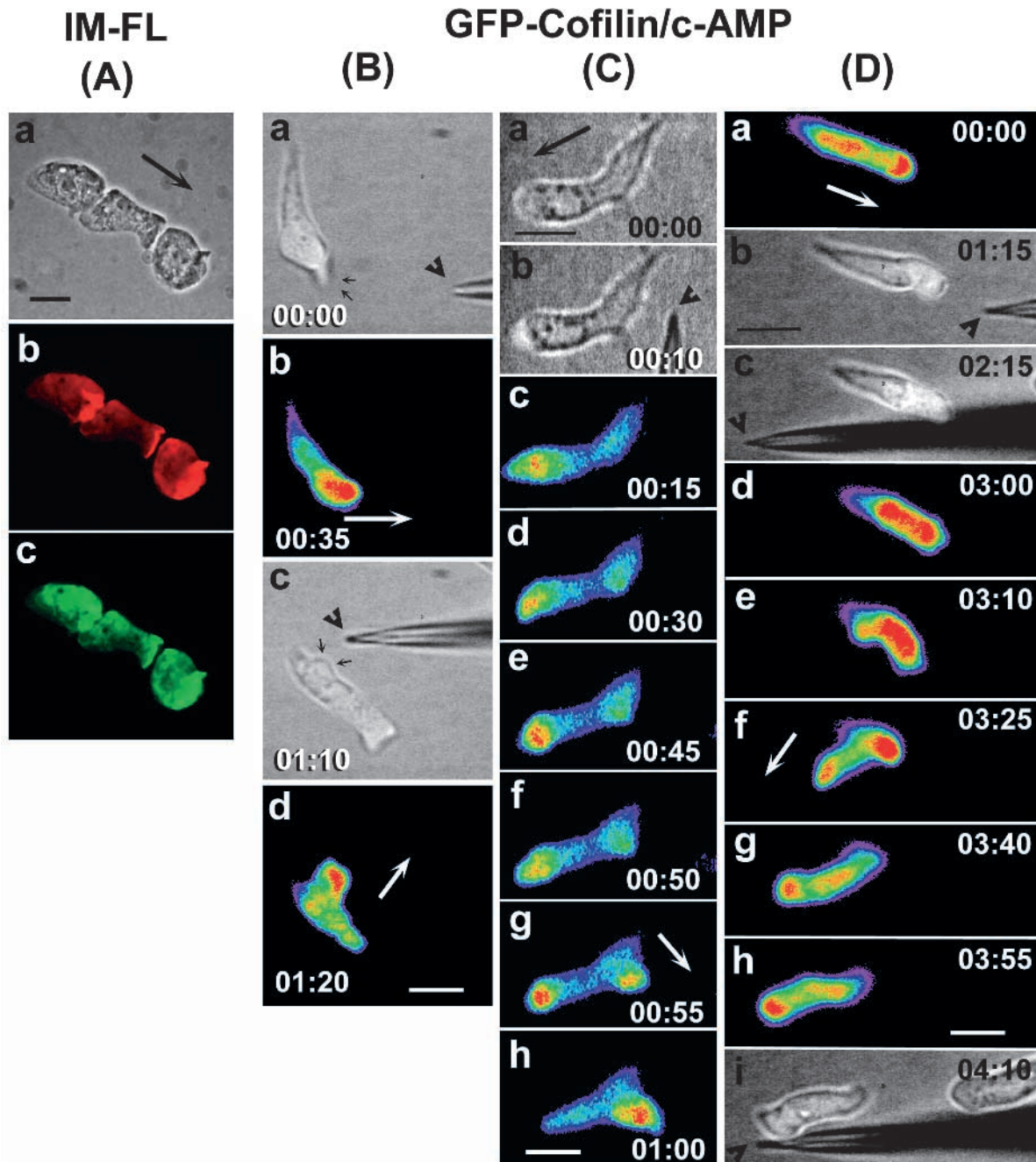


Fig. 8. Immunofluorescence localization of cofilin and live dynamics of GFP-cofilin during an induced chemotaxis to cAMP. (A) Phase-contrast (a) and double-staining immunofluorescence micrographs showing a high accumulation of actin (b) and cofilin (c) in leading pseudopodia. Note that the localization of cofilin is very similar to that of actin. The arrow indicates the direction of aggregation. (B-D) Live dynamics of GFP-cofilin in cells chemotactically activated with cAMP applied by the micropipette. In color images, the 8-bit fluorescence intensity is encoded by 8 colors. Red and purple, respectively, indicate the highest and lowest intensity. Note that the amoebae rapidly initiate the formation of a new lamella towards the source of cAMP (arrowheads), and GFP-cofilin integrates into these lamellae in about 30 seconds. Arrows indicate the direction of developing pseudopodia. Time scale, minutes:seconds. Bars, 5 μ m.

ciation with actin bundles during the F-actin remodeling processes.

We observed that actin filaments are organized into bundles only on the rim of crown-like structures which protrude from the dorsal cell cortex. The live cell observation showed that the crowns protrude and retract actively as the bundles assemble,

contract, and dissipate. Cofilin remains associated with the bundles during retraction. This evidence leads us to suggest that cofilin is involved in this cortical activity. Importantly, a recent study by Hacker et al. (1997) has demonstrated that the coronin plays a significant role in macropinocytosis of fluid-phase materials. The association of the two actin-binding

proteins, coronin (de Hostos et al., 1991) and cofilin (this study), with actin in the crown indicates that these actin-binding proteins probably work in concert to regulate the actin organization during macropinocytosis.

When the amoeba phagocytoses solid-phase materials, similar actin bundles are demonstrated to form in the cortex and attach to the material. These actin bundles are believed to produce forces to grasp and internalize the food materials. Cofilin appears to co-assemble with the actin bundles during this process. This provides another example of the physiological activity of cofilin in constructing actin bundles in a regulated manner.

It is conceivable that the actin cytoskeleton is responsible for producing forces necessary for the movement of the crown and phagocytic cups. Depletion of ATP by azide-treatment indeed suppresses movements of these structures (Persson et al., 1988; Pasternak et al., 1989). Myosin-I, a mechanochemical ATPase, is predominantly distributed in the lamellae and phagocytic cups (Fukui et al., 1989). Myosin-I has been shown to cross-link F-actin and contracts the actin gel in the presence of ATP (Fujisaki et al., 1985). Thus, it is reasonable to speculate that cofilin transforms the actin latticework made of F-actin and actin-crosslinking proteins such as myosin-I and/or α -actinin into bundles to provoke contraction of the actin gel.

Both immunofluorescence and GFP-cofilin observations clearly demonstrate that cofilin accumulates at the polar lamellae but not at the cleavage furrow during cytokinesis. This situation is remarkably similar to that of α -actinin (Fukui, 1993). In contrast, in murine and *Xenopus* cells, by immunofluorescence, cofilin has been reported to accumulate at the cleavage furrow during cytokinesis (Nagaoka et al., 1995; Abe et al., 1996). Although we have no clear explanation for the difference between *Dictyostelium* and vertebrate cells, an accumulation of cofilin at the cleavage furrow does not seem to be a prerequisite for the cytokinesis of *Dictyostelium*. The reason for this discrepancy is yet to be determined.

This study demonstrates that the local activation of cAMP-mediated chemotaxis induces the accumulation of cofilin at a projecting pseudopod within 1 minute. It has been previously demonstrated in *Dictyostelium* that ligand-activated cAMP receptors induce the activation of phospholipase-C via $G_{\alpha 2}$, an α -subunit of the trimeric G protein (Okaichi et al., 1992; Kumagai et al., 1989). The activated phospholipase-C has been shown to hydrolyze PIP₂ producing IP₃ and diacylglycerol within 5 seconds after the activation of the cAMP receptors (Bominaar and Van Haastert, 1994). In fact, we have shown that PIP₂ binds *Dictyostelium* cofilin and inhibits its interaction with actin, whereas IP₃ or diacylglycerol does not affect its activity (Aizawa et al., 1995). These observations suggest to us that activation of phospholipase-C via activated cAMP receptors may lead to the activation of cofilin by hydrolyzing cofilin-bound PIP₂, and the locally activated cofilin may consequently bind to F-actin, sever filaments, and ultimately help the short filaments form bundles in the presence of actin cross-linking proteins such as α -actinin.

In higher eukaryotes, cofilin is known to be functionally regulated by phosphorylation at its serine residue close to its amino terminus (Agnew et al., 1995; Moriyama et al., 1996). In contrast, in lower eukaryotes such as *S. cerevisiae* and *D. discoideum*, a phosphorylated form of cofilin appears to be absent (K. Iida and H. Aizawa, unpublished observations).

Therefore, we suspect that the hydrolysis of polyphosphoinositides such as PIP₂ might be responsible for the activation of cofilin in regulating the actin-based motile system in *Dictyostelium*.

Another actin-binding protein, coronin, has been also reported to accumulate dynamically into crowns of free-moving cells, phagocytic cups of vegetative cells, and leading edges of chemotactic cells (Gerisch et al., 1995; Maniak et al., 1995). Although cofilin (Yonezawa et al., 1985) and coronin (de Hostos et al., 1991) appear to be regulated by distinct mechanisms such as pH, phosphorylation, and binding with PIP₂, their temporal and spatial association with actin seem to share certain similarities. This feature may indicate the occurrence of a cooperative interaction of coronin and cofilin with actin filaments in regulating the actin architecture.

Overall, this study demonstrates that, in live *Dictyostelium*, cofilin assembles into the actin cytoskeleton in a temporally and spatially regulated manner. We interpret this dynamic as a reflection of the bona fide function of cofilin i.e. facilitating the remodeling of an actin lattice into functional bundles. Although other actin-binding proteins are also thought to be involved in this process, the role of cofilin seems crucial because its gene knockout has been proved to be lethal (Aizawa et al., 1995).

We thank Dr R. Y. Tsien for the generous gift of a vector encoding S65T-GFP. We thank Dr M. Sameshima for excellent scanning electron microscopy. Thanks are due to Dr K. Iida and Dr K. Moriyama for helpful discussion. We also thank I. Fukui for proof-reading the manuscript. This work was supported in part by a grant-in-aid from the Ministry of Education, Science and Culture of Japan to I.Y., and by grants from NIH GM39548 to Y.F.

REFERENCES

- Abe, H., Obinata, T., Minamide, L. S. and Bamburg, J. R. (1996). *Xenopus laevis* actin-depolymerizing factor/cofilin: A phosphorylation-regulated protein essential for development. *J. Cell Biol.* **132**, 871-885.
- Agnew, B. J., Minamide, L. S. and Bamburg, J. R. (1995). Reactivation of phosphorylated actin depolymerizing factor and identification of the regulatory site. *J. Biol. Chem.* **270**, 17582-17587.
- Aizawa, H., Sutoh, K., Tsubuki, S., Kawashima, S., Ishii, A. and Yahara, I. (1995). Identification, characterization, and intracellular distribution of cofilin in *Dictyostelium discoideum*. *J. Biol. Chem.* **270**, 10923-10932.
- Aizawa, H., Sutoh, K. and Yahara, I. (1996). Overexpression of cofilin stimulates bundling of actin filaments, membrane ruffling, and cell movement in *Dictyostelium*. *J. Cell Biol.* **132**, 335-344.
- Bamburg, J. R., Harris, H. E. and Weeds, A. G. (1980). Partial purification and characterization of an actin depolymerizing factor from brain. *FEBS Lett.* **121**, 178-182.
- Bominaar, A. A. and Van Haastert, P. J. M. (1994). Phospholipase C in *Dictyostelium discoideum*: Identification of stimulatory and inhibitory surface receptors and G-proteins. *Biochem. J.* **297**, 189-193.
- Bonner, J. T. (1947). Evidence for the formation of cell aggregates by chemotaxis in the development of the slime mold *Dictyostelium discoideum*. *J. Exp. Zool.* **106**, 1-26.
- Cooper, J. A., Cooper, J. D., Williams, R. J. and Pollard T. D. (1986). Purification and characterization of actophorin, a new 15,000-dalton actin-binding protein from *Acanthamoeba castellanii*. *J. Biol. Chem.* **261**, 477-485.
- de Hostos, E. L., Bradtke, B., Lottspeich, F., Guggenheim, R. and Gerisch, G. (1991). Coronin, an actin binding protein of *Dictyostelium discoideum* localized to cell surface projections, has sequence similarities to G protein beta subunits. *EMBO J.* **10**, 4097-4104.
- Fukui, Y. (1978). Intracellular actin bundles induced by dimethyl sulfoxide in interphase nucleus of *Dictyostelium*. *J. Cell Biol.* **76**, 146-157.

- Fukui, Y. and Yumura, S.** (1986). Actomyosin dynamics in chemotactic amoeboid movement of *Dictyostelium*. *Cell Motil. Cytoskel.* **6**, 662-273.
- Fukui, Y., Yumura, S. and Mori, H.** (1986). Agar overlay method: high-resolution immunofluorescence for the study of the contractile apparatus. *Meth. Enzymol.* **134**, 573-580.
- Fukui, Y., Lynch, T. J., Brzeska, H. and Korn, E. D.** (1989). Myosin I is located at the leading edges of locomoting *Dictyostelium* amoebae. *Nature* **341**, 328-331.
- Fukui, Y. and Inoué, S.** (1991). Cell division in *Dictyostelium* with special emphasis on actomyosin organization in cytokinesis. *Cell Motil. Cytoskel.* **18**, 41-54.
- Fukui, Y.** (1993). Toward a new concept of cell motility: Cytoskeletal dynamics in amoeboid movement and cell division. *Int. Rev. Cyt.* **144**, 85-127.
- Fukui, Y. and Inoué, S.** (1997). Amoeboid movement anchored by eupodia, new actin-rich knobby feet in *Dictyostelium*. *Cell Motil. Cytoskel.* **36**, 339-354.
- Fujisaki, H., Albanesi, J. P. and Korn, E. D.** (1985). Experimental evidence for the contractile activities of *Acanthamoeba* myosins IA and IB. *J. Biol. Chem.* **260**, 11183-11189.
- Gerisch, G., Albrecht, R., Heizer, C., Hodgkinson, S. and Maniak, M.** (1995). Chemoattractant-controlled accumulation of coronin at the leading edge of *Dictyostelium* cells monitored using a green fluorescent protein-coronin fusion protein. *Curr. Biol.* **5**, 1280-1285.
- Hacker, U., Albrecht, R. and Maniak, M.** (1997). Fluid-phase uptake by macropinocytosis in *Dictyostelium*. *J. Cell Sci.* **110**, 105-112.
- Hartwig, J. H. and Kwiatkowski, D. J.** (1991). Actin-binding proteins. *Curr. Opin. Cell Biol.* **3**, 87-97.
- Hatanaka, H., Ogura, K., Moriyama, K., Ichikawa, S., Yahara, I. and Inagaki, F.** (1996). Tertiary structure of destrin and structural similarity between two actin-regulating protein families. *Cell* **85**, 1047-1055.
- Hawkins, M., Pope, B., Maciver, S. K. and Weeds, A. G.** (1993). Human actin depolymerizing factor mediates a pH-sensitive destruction of actin filaments. *Biochemistry* **32**, 9985-9993.
- Iida, K., Iida, H. and Yahara, I.** (1986). Heat shock induction of intranuclear actin rods in cultured mammalian cells. *Exp. Cell Res.* **165**, 207-215.
- Iida, K. and Yahara, I.** (1986). Reversible induction of actin rods in mouse C3H-2K cells by incubation in salt buffers and by treatment with non-ionic detergents. *Exp. Cell Res.* **164**, 492-506.
- Iida, K., Moriyama, K., Matsumoto, S., Kawasaki, H., Nishida, E. and Yahara, I.** (1993). Isolation of a yeast essential gene, COF1, that encodes a homologue of mammalian cofilin, a low-Mr actin-binding and depolymerizing protein. *Gene* **124**, 115-120.
- Kumagai, A., Pupillo, M., Gundersen, R., Miake-Ley, R., Devreotes, P. N. and Firtel, R. A.** (1989). Regulation and function of G-alpha protein subunits in *Dictyostelium*. *Cell* **57**, 265-275.
- Laemmli, U. K.** (1970). Cleavage of structural proteins during the assembly of the head of bacteriophage T4. *Nature* **227**, 680-685.
- Mabuchi, I.** (1981). Purification from starfish eggs of a protein that depolymerizes actin. *J. Biochem. (Tokyo)* **89**, 1341-1344.
- Maciver, S. K., Wachsstock, D. H., Schwarz, W. H. and Pollard, T. D.** (1991). The actin filament severing protein promotes the formation of rigid bundles of actin filaments crosslinked with α -actinin. *J. Cell Biol.* **115**, 1621-1628.
- Maniak, M., Rauchenberger, R., Albrecht, R., Murphy, J. and Gerisch, G.** (1995). Coronin involved in phagocytosis: dynamics of particle-induced relocalization visualized by a green fluorescent protein Tag. *Cell* **83**, 915-924.
- McLaughlin, P. J., Gooch, J. T., Mannherz, H.-G. and Weeds, A. G.** (1993). Structure of gelsolin segment-1-actin complex and the mechanism of filament severing. *Nature* **364**, 685-692.
- Moon, A. L., Janmay, P. A., Louie, K. A. and Drubin, D. G.** (1993). Cofilin is an essential component of the yeast cortical cytoskeleton. *J. Cell Biol.* **120**, 421-435.
- Moon, A. and Drubin, D. G.** (1995). The ADF/cofilin proteins: stimulus-responsive modulators of actin dynamics. *Mol. Biol. Cell* **6**, 1423-1431.
- Moriyama, K., Iida, K. and Yahara, I.** (1996). Phosphorylation of Ser-3 of cofilin regulates its essential function of actin. *Genes to Cells* **1**, 73-86.
- Nagaoka, R., Abe, H., Kusano, K. and Obinata, T.** (1995). Concentration of cofilin, a small actin-binding protein, at the cleavage furrow during cytokinesis. *Cell Motil. Cytoskel.* **30**, 1-7.
- Nishida, E., Maekawa, S. and Sakai, H.** (1984). Cofilin, a protein in porcine brain that binds to actin filaments and inhibits their interactions with myosin and tropomyosin. *Biochemistry* **23**, 5307-5313.
- Nishida, E., Muneyuki, E., Maekawa, S., Ohta, Y. and Sakai, H.** (1985). An actin depolymerizing protein (destrin) from porcine kidney. Its action on F-actin containing or lacking tropomyosin. *Biochemistry* **24**, 6624-6630.
- Nishida, E., Iida, K., Yonezawa, N., Koyasu, S., Yahara, I. and Sakai, H.** (1987). Cofilin is a component of intranuclear and cytoplasmic actin rods induced in cultured cells. *Proc. Nat. Acad. Sci. USA* **84**, 5262-5266.
- Okaichi, K., Cubitt, A. B., Pitt, G. S. and Firtel, R. A.** (1992). Amino acid substitutions in the *Dictyostelium* G alpha subunit G alpha 2 produce dominant negative phenotypes and inhibit the activation of adenyl cyclase, guanylyl cyclase, and phospholipase C. *Mol. Biol. Cell* **3**, 735-747.
- Ono, S., Abe, H., Nagaoka, R. and Obinata, T.** (1993). Colocalization of ADF and cofilin in intranuclear rods of cultured muscle cells. *J. Muscle Res. Cell Motil.* **14**, 195-204.
- Pasternak, C., Spudich, J. A. and Elson, E. L.** (1989). Capping of surface receptors and concomitant cortical tension are generated by conventional myosin. *Nature* **341**, 549-551.
- Persson, R., Ahlstrom, E. and Fries, E.** (1988). Differential arrest of secretory protein transport in cultured rat hepatocytes by azide treatment. *J. Cell Biol.* **107**, 2503-2510.
- Pollard, T. D. and Cooper, J. A.** (1986). Actin and actin-binding proteins. A critical evaluation of mechanisms and functions. *Annu. Rev. Biochem.* **55**, 987-1035.
- Pollard, T. D.** (1993). Actin and actin binding proteins. In *Guidebook to the Cytoskeletal and Motor Proteins* (ed. T. Kreis and R. Vale), pp. 3-11. Oxford University Press, Oxford.
- Stossel, T. P., Chaponnier, C., Ezzel, R. M., Hartwig, J. H., Jamney, P. A., Kwiatkowski, D. J., Lind, S. E., Smith, D. B., Southwick, F. S., Yin, H. L. and Zaner, K. S.** (1985). Non-muscle actin binding protein. *Annu. Rev. Cell Biol.* **1**, 353-402.
- Spudich, J. A. and Watt, S.** (1971). The regulation of rabbit skeletal muscle contraction. I. Biochemical studies of the interaction of the tropomyosin-tropoanin complex with actin and the proteolytic fragments of myosin. *J. Biol. Chem.* **246**, 4866-4871.
- Sun, H. Q., Kwiatkowska, K. and Yin, H. L.** (1995). Actin monomer binding proteins. *Curr. Opin. Cell Biol.* **7**, 102-110.
- Sutoh, K.** (1993). A transformation vector for *Dictyostelium discoideum* with a new selectable marker bsr. *Plasmid* **30**, 150-154.
- Towbin, H., Staehelin, T. and Gordon, J.** (1979). Electrophoretic transfer of proteins from polyacrylamide gels to nitrocellulose sheets: procedure and some applications. *Proc. Nat. Acad. Sci. USA* **74**, 4350-4354.
- Uyeda, T. Q., Ruppel, K. M. and Spudich, J. A.** (1994). Enzymatic activities correlate with chimeric substitution at the actin-binding face of myosin. *Nature* **368**, 567-569.
- Vandekerckhove, J. and Vancompernelle, K.** (1992). Structural relationships of actin binding proteins. *Curr. Opin. Cell Biol.* **4**, 36-42.
- Yahara, I., Aizawa, H., Moriyama, K., Iida, K., Yonezawa, N., Nishida, E., Hatanaka, H. and Inagaki, F.** (1996). A role of cofilin/destrin in reorganization of actin cytoskeleton in response to stresses and cell stimuli. *Cell Struct. Funct.* **21**, 421-424.
- Yonezawa, N., Nishida, E. and Sakai, H.** (1985). pH control of actin polymerization by cofilin. *J. Biol. Chem.* **260**, 14410-14412.
- Yonezawa, N., Nishida, E., Iida, K., Yahara, I. and Sakai, H.** (1990). Inhibition of the interactions of cofilin, destrin and deoxyribonuclease I with actin by phosphoinositides. *J. Biol. Chem.* **265**, 8382-8386.
- Yumura, S., Mori, H. and Fukui, Y.** (1984). Localization of actin and myosin for the study of amoeboid movement in *Dictyostelium discoideum* using improved immunofluorescence. *J. Cell Biol.* **99**, 894-899.